PORE COMBINATION MODELING: EXTENDING THE HANAI-BRUGGEMAN EQUATION

M. T. Myers

Abstract

The technique of pore combination modeling (PCM) is extended to include conductive inclusions. Conductive inclusions are modeled similar to previously published work (Myers 1989) except that the Hanai-Bruggeman equation is used instead of the Archie equation. Models for laminated and dispersed clay conduction are developed which incorporate the effects of clay geometry. These models show that the conductivity is intimately related to the geometry of the clays for both the laminated and dispersed cases.

The model developed for dispersed clays explains the increase in the effective clay-counterion mobility with increasing salinity as a coupling between the conductivity of the clays and the conductivity of the brine. It also demonstrates that the shape of the conductivity curve depends on the ratio of intergranular to isolated clay porosity.

D

Introduction

The depositional history and lithology of rocks are important factors in determining their petrophysical properties. Rocks exhibit structure on many different length scales. Such as the different conduction properties of laminated and dispersed clays. Including this type of structure is important to accurately model rock properties. This is done by a simple extension of the Hanai-Bruggeman equation.

The Hanai-Bruggeman equation (Bruggeman 1932, Hanai 1968) is based on an effective medium approximation. In this approximation as inclusions are added to a host it is assumed that the host properties may be approximated by the average properties of the mixture. Longer length scales are therefore implicitly included as more material is added(Merideth, Tobias 1962). We use this shifting of length scales to advantage in developing models. It determines the order the geologic features are added, those with longer length scales are added after those with shorter ones.

In the derivation of the Hanai-Bruggeman equation a differential equation is obtained for the dielectric constant of a mixture of small amounts of an inclusion in a host. This equation is integrated over the addition of a single inclusion to obtain the Hanai-Bruggeman equation. We allow for multiple distinct lithology changes by successive application of the differential form of the equation. Starting with the first inclusion introduced to the pure host, similar integrations are performed as each component is added. At each integration step we start from the conditions left at the end of the previous step

using the appropriate conductivities and shapes associated with the porosity change:

$$\int_{\sigma_{h,i,..,o}}^{\sigma_{h,i,..,o,p}} \left(\frac{1}{\sigma-\sigma_p} - \frac{L_p}{\sigma}\right) d\sigma \quad + \cdots + \int_{\sigma_h}^{\sigma_{h,i}} \left(\frac{1}{\sigma-\sigma_i} - \frac{L_i}{\sigma}\right) d\sigma$$

$$= \int_{{}^h\phi_{h,i,..,o}}^{{}^h\phi_{h,i,..,o,p}} \frac{d\phi}{\phi} + \cdots + \int_{1}^{{}^h\phi_{h,i}} \frac{d\phi}{\phi} \qquad (1)$$

Where σ_h is the conductivity of the host, σ_i the conductivity of the inclusion and $\sigma_{h,i}$ is the conductivity of the host and impurity. L_i is the depolarization ratio, a geometrical factor related to the shape of the inclusion, ${}^h\phi_{h,i}$ is the volume fraction of the host when host and inclusion are present. The superscripts are the volumes of the components of the host, the subscripts the volumes of the host and impurities. Since the volume of the mixture changes we need to keep track of all the volumes.

If σ_i is equal to zero then the Hanai-Bruggeman equation reduces to the Archie equation (Sen, et. al. 1981). Equation (1) therefore extends the Archie equation, and therefore pore combination modeling (PCM) to include the addition of conductive inclusions. The Hanai-Bruggeman equation has been suggested to model the conductive properties of rocks, (Bussian 1983, Sen 1980) what we add is a procedure to include specific geologic features to these models. This is accomplished by integrating equation (1) adding each geologic feature, with the ordering determined by the length scale associated with that feature.

We will show this integration in detail for specific examples, starting with simple situations, the addition of nonconducting inclusions. We then discuss the more complicated situation where the inclusions are conducting. This allows us to explicitly demonstrate the techniques and show some useful approximations along the way.

Non-conducting inclusions

Mixture of nonconducting inclusions with different shapes

In this section we integrate equation (1) for nonconducting inclusions with different shapes. Although the empirical derivation of these results has been previously published (Myers 1989) the details are instructive and will help to clarify the connection between this and the earlier work.

Add oil:

Oil drops with an effective shape determined by L_o are added to the host brine.

$$(1-L_o)\int_{\sigma_w}^{\sigma_{w,o}}\frac{d\sigma}{\sigma} = \int_{1}^{{}^{w}\phi_{w,o}}\frac{d\phi}{\phi}$$

or

$$\sigma_{w,o} = \sigma_w\cdot({}^{w}\phi_{w,o})^{n} = \sigma_w\cdot S_w^{\,n} \qquad (2)$$

Where $n=1/(1-L_o)$ and ${}^{w}\phi_{w,o}$ is the volume of the brine normalized to the volume of brine and oil (i.e., the water saturation, S_w).

Add nonconducting grains with shape L_{g1}:

Nonconducting grains with the shape $L=L_{g1}$ are added to the oil water mixture:

$$(1-L_{g1})\int_{\sigma_{w,o}}^{\sigma_{w,o,g1}}\frac{d\sigma}{\sigma} = \int_{{}^{w}\phi_{w,o}}^{{}^{w}\phi_{w,o,g1}}\frac{d\phi}{\phi}$$

or

$$\sigma_{w,o,g1} = \sigma_{w,o}\cdot({}^{w,o}\phi_{w,o,g1})^{\lambda_{g1}} = \sigma_w\cdot S_w^{\,n}\phi^{\lambda_{g1}} \qquad (3)$$

where $\lambda_{g1}=1/(1-L_{g1})$ and ${}^{w,o}\phi_{w,o,g1}$ is the fraction of water and oil normalized to the total bulk volume, i.e. the porosity. This is the Archie equation including the saturation dependence, which is a special case of the PCM integration scheme.

Add nonconducting grains with shape L_{g2}:

Add grains with the shape, $L=L_{g2}$ to the mixture of water, oil, and grains:

$$(1-L_{g2})\int_{\sigma_{w,o,g1}}^{\sigma_{w,o,g1,g2}}\frac{d\sigma}{\sigma} = \int_{{}^{w}\phi_{w,o,g1}}^{{}^{w}\phi_{w,o,g1,g2}}\frac{d\phi}{\phi}$$

or

$$\sigma_{w,o,g1,g2} = \sigma_{w,o,g1}\cdot({}^{w,o,g1}\phi_{w,o,g1,g2})^{\lambda_{g2}} \qquad (4)$$

Where λ_{g2} equals $1/(1-L_{g2})$.

Write in terms of petrophysical parameters:

Since the volume of the host and materials is changing with the addition of each component, the meaning of the equations is clearer when they are written in terms of more common petrophysical parameters.

$$^{w,o}\phi_{w,o,g1} = {}^{w,o}\phi_{w,o,g1,g2} / {}^{w,o,g1}\phi_{w,o,g1,g2} = \phi/(\phi + V_{g1}) = \phi/\phi_o \qquad (5)$$

Where ϕ is the fraction of water and oil normalized to the total volume, V_{g1} is the volume fraction of grain one normalized to total bulk volume and $\phi+V_{g1}$ is the porosity when just grain two is present. In terms of these parameters the equation for the conductivity is:

$$\sigma = \sigma_{w,o,g1,g2} = \sigma_w \cdot S_w^n \cdot \phi_o^{\lambda_{g2}} \cdot (\phi/\phi_o)^{\lambda_{g1}} \qquad (6)$$

The size dependence is implied by the order of integration. The larger particles have shape given by L_{g2}. If the shapes are the same, then $\lambda_{g1}=\lambda_{g2}$, and equation (6) reduces to the Archie equation.

Isolated porosity

Addition of isolated porosity is similar to above except that the porosity is increased in the second step. We compute the effects on the conductivity of removing a grain with shape L_i:

Add the grains:

$$(1-L_g)\int_{\sigma_w}^{\sigma_{w,g}} \frac{d\sigma}{\sigma} = \int_{1}^{{}^{w}\phi_{w,g}} \frac{d\phi}{\phi}$$

or

$$\sigma_{w,g} = \sigma_w \cdot {}^{w}\phi_{w,g}^{\lambda_g} \qquad (7)$$

Add the isolated porosity:

$$(1-L_i)\int_{\sigma_{w,g}}^{\sigma_{w,g,i}} \frac{d\sigma}{\sigma} = \int_{{}^{w}\phi_{w,g}}^{{}^{w,i}\phi_{w,g,i}} \frac{d\phi}{\phi}$$

or

$$\sigma = \sigma_{w,g,i} = \sigma_{w,g} \cdot ({}^{w,i}\phi_{w,g,i} / {}^{w}\phi_{w,g})^{\lambda_i}$$

$$= \sigma_w \cdot \phi_g^{\lambda_g} \cdot (\phi/\phi_g)^{\lambda_i} \qquad (8)$$

Where ϕ_g is the interparticle porosity ($\phi_g = {}^w\phi_{w,g}$) and is less than the total porosity ϕ. If we write the equation in terms of porosities normalized to the entire bulk volume of the sample we obtain.

$$\sigma = \sigma_w \cdot \phi_m^{\lambda_g} \cdot (\phi/\phi_m)^{\lambda_i} \cdot (1-\phi_i)^{\lambda_i-\lambda_g} \qquad (9)$$

Where ϕ_m is the interparticle porosity normalized to the entire bulk volume ($\phi_m = {}^w\phi_{w,g,i}$), and ϕ_i is the volume fraction of isolated porosity ($\phi_i = {}^i\phi_{w,g,i}$). Writing equation (8) in ϕ_m adds the $1-\phi_i$ term. This reflects the reduced volume fraction of interparticle porosity as you add isolated porosity.

Saturation dependence for bi-modal pore systems

The saturation dependence for isolated porosity depends on the pore system the oil enters. This saturation dependence may be modeled by reducing the porosity of the appropriate pore system by the volume of oil added. If oil is added to the interparticle porosity this also reduces the current through the isolated pore system and results in large saturation exponents. When oil is added to the isolated porosity there is relatively little effect on the conductivity. These saturation effects have been experimentally demonstrated (Swanson 1986) and discussed in detail elsewhere (Myers 1989).

Discussion of the models for non-conducting inclusions

These models include the simplest effects due to pore geometry in conductivity models. But even though they cover a surprising amount of the effects seen in the literature, they are really only starting points. For example, in carbonates sometimes the intergranular porosity is constant while the vuggy porosity is changing through diagenesis. Using this geologic information a model for the conductivity may be developed. PCM is a general framework for the construction of such models.

Adding Conducting Inclusions

Laminated clays

Consider the case of a clean sand interbedded with clay laminations. To calculate the model for such a system we integrate equation (1) over two types of inclusions. The conducting inclusions, the clay laminations, are added second because by definition they are connected on length scales larger than a grain size.

Add oil and nonconducting particles:

As in equation (3), we get the Archie equation for the sand.

$$\sigma_{w,o,g} = \sigma_{w,o}({}^{w,o}\phi_{w,o,g})^{\lambda_g} \tag{3}$$

Adding the clay:

$$\int_{\sigma_{w,o,g}}^{\sigma_{w,o,g,c}} \frac{d\sigma}{\sigma-\sigma_c} - L_c \int_{\sigma_{w,o,g}}^{\sigma_{w,o,g,c}} \frac{d\sigma}{\sigma} = \int_{{}^{w}\phi_{w,o,g}}^{{}^{w}\phi_{w,o,g,c}} \frac{d\phi}{\phi} \tag{10}$$

which gives

$$\left(\frac{\sigma_{w,o,g,c} - \sigma_c}{\sigma_{w,o,g} - \sigma_c}\right) \cdot \left(\frac{\sigma_{w,o,g,c}}{\sigma_{w,o,g}}\right)^{L_c} = {}^{w,o,g}\phi_{w,o,g,c} \tag{11}$$

Rewriting equations (3) and (10) in terms of more familiar parameters gives:

$$\sigma_s = \sigma_w S_w^n \phi_s^{\lambda_g} \tag{12}$$

$$\left(\frac{\sigma - \sigma_c}{\sigma_s - \sigma_c}\right) \cdot \left(\frac{\sigma}{\sigma_s}\right)^{-L_c} = V_s \tag{13}$$

Where $\phi_s = {}^{w,o}\phi_{w,o,g}$ is the interparticle porosity (the amount of water and oil normalized to the volume of the water, oil and grains), and $V_s={}^{w,o,g}\phi_{w,o,g,c}$ and $\sigma_s = \sigma_{w,o,g}$ are the volume fraction and the conductivity of the sand. Equations (12) and (13) are a Hanai-Bruggeman combination of the conductivity of the sand with the conductivity of the clay laminae.

Series and parallel models

Laminated sand-clay models typically take the form of parallel and series addition of the conductivities of the sand and clay. The proposed model is a generalization of this, setting $L_c=0$ in equation (13) and solving for the conductivity gives.

$$\sigma = V_s \cdot \sigma_s + (1-V_s) \cdot \sigma_c \tag{14}$$

While setting $L_c=1$ gives

$$1/\sigma = V_s/\sigma_s + (1-V_s)/\sigma_c \tag{15}$$

Equations (14) and (15) are parallel and series models for the conductivity of the mixture of clay and sand. The clay is in parallel or series with the mixture of brine, oil, and sand grains indicating the averaging assumptions that have gone into this order of integration. Intermediate values of L_c in equation (13) imply

that the conductivity model lies somewhere in between series and parallel models.

Approximating the Hanai-Bruggeman equation

For intermediate values of L we can approximate the Hanai-Bruggeman equation to arrive at a simpler expression with more intuitive appeal. Using equation (10) as an example, we multiply and divide by σ in the first term to obtain:

$$\int_{\sigma_s}^{\sigma} \left(\frac{\sigma}{\sigma-\sigma_c}\right) \frac{d\sigma}{\sigma} - L_c \int_{\sigma_s}^{\sigma} \frac{d\sigma}{\sigma} = \int_{\phi_s}^{\phi} \frac{d\phi}{\phi} \qquad (16)$$

If we make the approximation that $\sigma/(\sigma-\sigma_c)$ is constant, we can remove it from the integral. This is exact if the conductivity of the host is equal to the conductivity of the inclusion. Then conductivity of the mixture is unchanged by the addition of the inclusion. The approximation is reasonable when the conductivity of the inclusion is much less than mixture conductivity (adding nonconducting inclusions) or for small volumes of inclusions. It breaks down when the conductivity of the mixture changes rapidly with the addition of the inclusion. This occurs in two regions, for $\sigma_s<<\sigma_c$ with $L\approx 0$ and for $\sigma_s>>\sigma_c$ with $L\approx 1$. In these regions the appropriate series or parallel models may be used as described above. Applying the approximation to equation (10) gives:

$$\sigma = \sigma_s \cdot V_s^{\lambda_{c1}} \qquad (17)$$

where

$$\lambda_{c1} = \frac{\sigma_s - \sigma_c}{L_c \cdot \sigma_c + (1-L_c) \cdot \sigma_s} \qquad (18)$$

This approximate form is analogous to the Archie equation with the sand playing the role of the brine, but with an exponent that depends on the conductivities of both the clay and sand. The exponent depends on these conductivities because the effective tortuosity for electrical flow of the pore system depends on the conductivity difference of the clay and the sand. This exponent λ_{c1} is zero when the conductivity of the clay is equal to the conductivity of the sand i.e. the tortuosity doesn't change. The exponent is negative if the inclusion is more conductive than the host and positive if it is less conductive.

Salinity dependence of laminated clays

Figures (1a) and (1b) show the salinity dependence of the laminated sand model on the volume of sand and the effects of clay geometry. For both figures start we assume $\phi_s=.20$, $L_c=.5$, $\sigma_c=.5$,

V_s=.75, L_s=.5. Varying the volume of sand and brine conductivity gives figure (1a), varying clay geometry and brine conductivity gives figure (1b).

In figure (1a) the volume fraction of sand has been varied from all sand to all clay. The conductivity of the mixture at high salinity approaches a linear dependence on the brine conductivity. The rate of increase is the largest for clean sands and zero for pure clay varying smoothly between these limits with the volume of sand. This suggests that C_o-C_w plot of this type along with the appropriate model is useful for determining net sand ratios in samples. The linear portion of the curve extrapolated to zero brine conductivity can be solved for this ratio.

In figure (1b) only the clay geometry is varied. For a parallel geometry the clay contribution to the total conductivity does not depend on the brine conductivity. For any other geometry the contribution of the clays to the total conductivity depends on the brine conductivity. The coupling of the two conductivities forces the conductivity of the mixture goes to zero at low salinities.

When the conductivity of the sand (mixture of the brine and the grains) gets high enough to equal the conductivity of the clay the conductivity of the mixture is independent of geometry. The coupling of the sand and the clay conductivity therefore depends on the geometry of the clays. We will see an analogous effect for the salinity dependence of dispersed clays discussed later.

Saturation dependence of the laminated clays

In figure (2a) we show the dependence of saturation on the volume fraction of sand in the sample. The conductivity of the pure clay is independent of oil saturation while for the pure sand the saturation dependence follows the Archie relation.

In figure (2b) the saturation dependence of the laminated clay model is plotted as a function of the geometry of the clays. The saturation dependence in the model amounts to replacing the conductivity of the brine with the conductivity of the brine and oil ($\sigma_w \rightarrow \sigma_w S_w^n$). The discussion for the salinity dependence therefore applies here as well.

Dispersed clays

In the model for dispersed clays equation (1) is again integrated twice, this time the first inclusion is conducting. This model differs from the laminated clays only in the order in which the conductive component is added. A dispersed clay is connected over length scales smaller than a pore (roughly given by the grain size) so they are added before the grains. Integrating equation (1) with this ordering gives:

$$\left(\frac{\sigma_{wc} - \sigma_c}{\sigma_w - \sigma_c}\right) \cdot \left(\frac{\sigma_{wc}}{\sigma_w}\right)^{-L_c} = \frac{\phi}{\phi + V_c} \tag{19}$$

$$\sigma = \sigma_{wcg} = \sigma_{wc} \cdot (\phi + V_c)^{\lambda_g} \tag{20}$$

and approximating equation (19) we get.

$$= \sigma_w \, \phi_o^{\lambda_g} \cdot (\phi/\phi_o)^{\lambda_{cd}} \tag{21}$$

Where $\phi_o=\phi+V_c$ is the porosity of the rock without the clay and λ_{dc} depends on the conductivities of the rocks components:

$$\lambda_{cd} = \frac{\sigma_w - \sigma_c}{L_c \cdot \sigma_c + (1-L_c) \cdot \sigma_w} \tag{22}$$

Figure (3a) is the plot of the salinity dependence implied by equations (18) and (19) (the C_o-C_w curve) as a function of the volume of clay added. These curves were calculated using similar parameters (ϕ_s=.20, L_c=0.5, σ_c=0.5, V_c=.05, L_g=0.5) to those for laminated sands to allow direct comparison. The isoconductivity point for dispersed clays occurs when the conductivity of the clay is equal to the conductivity of the brine. For laminated clays the isoconductivity point occurred when the clay conductivity equaled the sand conductivity. The means that the curvature in the dispersed clay curve occurs at much lower salinities when compared to the equivalent plot for laminated clays.

In the dispersed clay model the conductivity of the shaly sand is expressed in terms of the volume of clay and the clay conductivity. In the next section we discuss the connection of this model with Q_v based models.

Relation to Q_v based models

For the purposes of discussion it is convenient to factor the expression for λ_{cd} into two terms, one of which contains all the geometry dependence.

$$\lambda_{cd} = \lambda_L \cdot \sigma_n = (1/(1-L \cdot \sigma_n)) \cdot \sigma_n \tag{23}$$

where $\sigma_n=(\sigma_w-\sigma_c)/\sigma_w$ is the normalized conductivity difference between the brine and the clay. The first order expansion of equation (20) in terms of σ_n gives:

$$\sigma = \sigma_w \cdot \phi_o^{\lambda_g} \cdot [1 + \sigma_n \cdot (\phi - \phi_o)/\phi_o]^{\lambda_L} \quad (24)$$

Substituting for σ_n and further algebra gives.

$$\sigma = \sigma_w \cdot \phi_o^{\lambda_s} \cdot (\phi/\phi_o)^{\lambda_L} \cdot [1 + (\sigma_c/\sigma_w) \cdot (\phi_o - \phi)/\phi]^{\lambda_L} \quad (25)$$

To see the connection with Q_v based models we rewrite σ_c as $\mu_c \cdot N \cdot e$, where μ_c is the mobility of the clay counter-ions, N is the concentration of counter-ions per unit volume of clay and e is a unit charge. Then

$$\sigma_c \cdot (\phi_o - \phi)/\phi = \mu_c \cdot e \cdot N \cdot (\phi_o - \phi)/\phi = \sigma^e \cdot Q_v \quad (26)$$

Where σ^e is the equivalent conductivity of the clay counter-ions and Q_v is the concentration of the charge in the pore space measured in equivalents/liter. The ratio of the porosities changes the normalization of the concentration of charge from the volume of clays to the volume of pore space. Substituting into equation (25) gives:

$$\sigma = \sigma_w \cdot \phi_o^{\lambda_g} \cdot (\phi/\phi_o)^{\lambda_L} \cdot [1 + (\sigma^e/\sigma_w) \cdot Q_v]^{\lambda_L} \quad (27)$$

Assuming a parallel model(λ_L=1) gives

$$\sigma = \phi^{m^*} \cdot [\sigma_w + \sigma^e \cdot Q_v] \quad (28)$$

Which is the Waxman-Smits equation (Waxman and Smits, 1968), where we have rewritten $\phi_o^{\lambda_g} \cdot (\phi/\phi_o)^{\lambda_L}$ as ϕ^{m^*}. Even if a parallel model is not assumed we still get the Waxman-Smits equation in the high salinity limit. If $\sigma_w >> \sigma_c$, $\lambda_L \approx 1/(1-L_c) = \lambda_c$ and the clay conduction term in equation (27) is small, so again expanding:

$$\sigma = \phi^{m^*}[\sigma_w + \lambda_c \cdot \sigma^e \cdot Q_v]$$

$$= \phi^{m^*}[\sigma_w + B_{max} \cdot Q_v] \quad (29)$$

B_{max} is the high salinity limit of the effective clay counter-ion conductivity(Waxman,Smits 1968). The effective clay counter-ion mobility $B_{max} = \lambda_c \cdot \sigma^e$ is a function of the clay geometry. The PCM based dispersed clay model represents an extension to Waxman-Smits equation which allows clay geometry to be included.

The derivation of equation (29) also explains why Q_v is the appropriate parameter for shaly sand analysis. There are two conducting materials present in the pores of the rock, the clays and the brine. The total conductivity depends on their relative contributions. The clay contribution is measured by the CEC, the the brine contibution by the porosity. The ratio of these is Q_v, which therefore gives the relative contributions.

Salinity dependence implied by clay geometry

From the above discussion we see that the clay geometry is an important factor in determining the conductivity behavior of dispersed clays. A parallel geometry (L_c=0) implies that there is no salinity dependence due to the λ_L term. Otherwise, there is a salinity dependence due to just the clay geometry. Figure (3a) is the C_o-C_w curve for dispersed clay varying only the clay geometry.

The mechanism for this salinity dependence is explained as a coupling between the conductivity of the clays and the brine. Since by definition dispersed clay exists in discrete sites the clay counter-ions have to physically leave the clay surface to contribute to the total conduction. Only for a parallel geometry are the two conduction mechanisms completely decoupled. It is "only in each single pore or section of a pore that the rock surface and the pore fluid may be considered parallel conductors" (Van Olphen, Waxman, 1958).

This means that for the clays to remain electrically neutral, ions from the pore fluid have to replace the ions leaving the clay surface i.e. the brine conductivity is coupled to the clay conductivity. This coupling is the mechanism for the salinity dependence, the fewer the number of ions that are present in the brine to couple on and off the clays the fewer the number of clay counter-ions that can contribute to conduction.

The coupling mechanism explains the increase in the effective mobility of the of the clay counter-ions as the conductivity of the brine increases. This is thought to be the major component in the salinity dependence of the effective clay counter-ion mobility, rather than effects due to the presence of the double layer. For a surface of constant charge density (which is appropriate for clays) the expectation is that the mobility should decrease with increasing salinity. There is no increase in total charge as there would be if the boundary condition was a constant surface potential e.g. quartz. "Therefore, if there is any change in specific surface conductance of clay with electrolyte concentration, this change cannot be an increase, as for glass, but must be a decrease." (Van Olphen, Waxman, 1958). Since shaly sand conductivity measurements show an increase in the effective clay counter-ion mobility, these effects due to the double layer must be relatively small. In the present model they are ignored and a constant mobility for the clay counter-ions is assumed.

B_{max} is effected by geometry because of the competing effects of geometry and conduction. As explained above, as the brine conductivity increases, the effective conductivity of the clays increases. When the brine conductivity gets sufficiently high (the isoconductivity point) the conductivity of the clays is equal to the conductivity of the brine, and the conductivity of the mixture is independent of clay geometry. Consequently, the larger the

value for L_c, the more the effective conductivity of the clays has to increase to make up for the decrease in conductivity due to geometry.

Saturation dependence of dispersed clays

When we add oil in the above model, a choice has to be made as to whether it should be before or after the clays. Adding the oil before the clays gives:

$$\sigma_{wo} = \sigma_w \cdot S_w^n$$

$$\left(\frac{\sigma_{woc} - \sigma_c}{\sigma_w - \sigma_c}\right) \cdot \left(\frac{\sigma_{woc}}{\sigma_w}\right)^{-L_c} = \frac{\phi}{\phi + V_c} \qquad (30)$$

$$\sigma = \sigma_{wocg} = \sigma_{woc} \cdot (\phi + V_c)^{\lambda_g} \qquad (31)$$

Examining equations (30) and (31) we find that the effect of adding oil is to replace with $\sigma_w S_w^n$. If the clays are put in before the oil we get:

$$\left(\frac{\sigma_{wc} - \sigma_c}{\sigma_w - \sigma_c}\right) \cdot \left(\frac{\sigma_{wc}}{\sigma_w}\right)^{-L_c} = \frac{\phi \cdot S_w}{\phi \cdot S_w + V_c} \qquad (32)$$

$$\sigma_{wco} = \sigma_{wco} \cdot (\phi \cdot S_w + V_c)^{\lambda_g} \qquad (33)$$

Where we have assumed the geometry of the oil and sand grains is the same (λ_g=n). Comparison of these equations with the brine saturated case shows that ϕ has been replaced with $\phi \cdot S_w$.

These substitutions are a result of the ordering of the integrations. In deriving equations (30) and (31) we assumed the clays and grains saw only the average properties of the brine and oil, therefore the saturation change is equivalent to changing the conductivity of the brine($\sigma_w \rightarrow \sigma_w \cdot S_w^n$).

When we added the oil after the clay the oil effects the conductivity the same as reducing the porosity ($\phi \rightarrow \phi \cdot S_w$). By definition a dispersed clay is connected only over length scales smaller than an average pore size. Therefore the porosity reduction assumption is appropriate. This is consistent with the published data(Hill, Milburn 1956) and with the assumptions made in the Waxman-Smits equation($Q_v \rightarrow Q_v/S_w$)(Waxman, Thomas 1974).

Figure (3a-b) are plots of the saturation dependence predicted by equations (32) and (33). The resistivity index versus

saturation ($I-S_w$) plot is independent of the geometry of the clays. This occurs because the clay-brine mixture conductivity is independent of oil saturation. This value is normalized out of the $I-S_w$ curve. The amount of curvature does depend on the volume of clay. The larger the volume of clay the more curvature the plot exhibits.

Bi-modal clay model

To compare the dispersed clay model with data we need to include an accurate expression for the conductivity of the clay sites which include their porosity. We model the conduction of a clay site as:

$$\sigma_c = \phi_{cs}^{\lambda_{cs}} \cdot (\sigma_w + \sigma^e \cdot CEC_v/\phi_{cs}) \qquad (34)$$

Where λ_{cs} is the lithology exponent for the clay site, ϕ_{cs} the porosity of the clay site, σ^e is the equivalent conductivity of the clay counter-ions, and CEC_v is the cation exchange capacity per unit volume of the clay. The individual clay sites conduct similar to a sand but with the effective salinity increased by the number of exchange-ions associated with the clay. Using this expression in equations (19) and (20) we obtain:

$$\left(\frac{\sigma_{wc} - \sigma_c}{\sigma_w - \sigma_c}\right) \cdot \left(\frac{\sigma_{wc}}{\sigma_w}\right)^{-L_c} = \frac{\phi_i}{\phi_i + V_c} \qquad (35)$$

$$\sigma = \sigma_{wcg} = \sigma_{wc} \cdot (\phi_i + V_c)^{\lambda_g} \qquad (36)$$

Comparison reveals that ϕ has been replaced by $\phi_i = \phi - V_c \cdot \phi_{cs}$, the intergranular porosity. The intergranular porosity plays the same role as the total porosity in the earlier equations. Expanding in the high salinity limit gives:

$$\sigma = \phi_{io}^{\lambda_g} \cdot (\phi_i/\phi_{io})^{\lambda_c} \cdot [\sigma_w \cdot (1 + \lambda_c \cdot V_c \cdot \phi_{cs}^{\lambda_{cs}}/\phi_i) + \lambda_c \cdot V_c \cdot \phi_{cs}^{\lambda_{cs}-1} \cdot \sigma^e \cdot CEC_v/\phi_i] \qquad (37)$$

Where $\phi_{io} = \phi_i + V_c$. This is linear in σ_w, substituting for V_c gives the expression for the slope,

$$\phi^{m*} = \phi_{io}^{\lambda_g} \cdot (\phi_i/\phi_{io})^{\lambda_c} \cdot (1 + \lambda_c \cdot \phi_{cs}^{\lambda_{cs}-1} \cdot (\phi - \phi_i)/\phi_i)$$

which is the first order expansion of:

$$\phi^{m*} \approx \phi_{io}^{\lambda_g} \cdot (\phi_i/\phi_{io})^{\lambda_c} \cdot (\phi/\phi_i)^{<\lambda_c>} \qquad (38)$$

where

$$<\lambda_c> = \lambda_c \cdot \phi_{cs}^{\lambda_{cs}-1} \qquad (39)$$

The last two terms in equation (38) are the same as equation (7) for isolated porosity. The exponent for the isolated porosity is given by equation (39). This exponent depends on both the distribution of clays (given by λ_c) and the complexity of the pore system in the clays (given by $\phi_{cs}^{\lambda_{cs}-1}$). Factoring this term and substitution for Q_v gives:

$$\sigma = \phi^{m^*} \cdot [\sigma_w + <\lambda_c> \cdot (\phi/\phi_i) \cdot \sigma^{1-<\lambda_c>} \cdot Q_v] \qquad (40)$$

The formation factor for the clay counter-ions and the brine are now different. This is a result of the bi-modal model and the isolated nature of the clays. We will see the effects of the difference in formation factors when this model is compared to shaly sand data.

Saturation dependence

The bi-modal nature of a shaly sand also effects the I-Sw curve. The pore system which the oil enters determines its effects on the conductivity. The saturation dependence may be modeled by reducing the appropriate porosity by the volume of oil that enters that pore system. The details of the I-S_w curve therefore depend on the capillary pressure curve for the sample under study.

Comparison of bi-modal model with shaly sand data

The shaly sand literature is particularly sparse when it comes to shaly sand measurements. The only complete data set is still the Waxman-Smits group II samples (Waxman, Smits 1968). We will use this data set to compare with the bi-modal clay model.

The values for the geometric parameters come from comparison of m^* values with point count data (Myers 1989). They are λ_g=1.72 and $<\lambda_c>$=.72. For simplicity λ_c was assumed to be equal to λ_{cs} (i.e. we are assuming the clays look the same on these two length scales) which using equation (39) gives them both a value of 3.2. The porosity of the clay was assumed to be 50%.

The equation for isolated porosity is inverted using the measured m^* values to obtain clay volumes for the group II samples. In figure (5) we plot the volumes of clay obtained against the measured CEC values. The clay types and amounts of clay were obtained from the Waxman-Smits paper. The lines in figure (5) are the fits for the proportionality constant, which relates the volume of the clay to its CEC ($V_c=\alpha \cdot Q_v \cdot \phi$). The best fit to this data gives α=.90 for montmorillonite and α=2.0 for the other clays. Where α has units of liter/equiv.. The data available did not justify defining individual values for the other clays present. This change in the value with clay type is in the direction expected

i.e. a larger CEC per unit volume of clay for montmorillonite than for the other clays.

The best fit for the equivalent conductivity of the clay counter-ions is σ^e=.045 cm^2 $equiv^{-1}$ ohm^{-1}, close to the Waxman-Smits group II value (B_{max}=.046)(Waxman, Smits 1968). This implies that the temperature effects may be accounted for using the published values of B_{max} (Waxman and Thomas 1974).

In figure (6a) we plot the comparison between the calculated values of the clay conduction and the measured values. The parameters that change are the sample porosity, Qv and α when the clay type changes. This comparison is very good demonstrating that the contribution due to the clays is accurately being accounted for. In figure (6b) we show the comparison between the calculated and measured values of m^*. Some of the deviations in this plot are believed to be due to the presence of clay laminae. Laminae cause large increases in Q_v with small effects on m^*.

Effects due to bi-modal porosity

Figure (7a) is a plot of the values for the percent clay conduction, δ, for selected Waxman-Smits group II sample data(Waxman, Smits 1968). Every other sample is plotted in order of increasing shaliness for the samples containing only kaolinite. The parameter δ measures the percentage of the maximum clay conduction the clays contribute at any salinity. A value of one implies the clays are fully conducting, a value of zero implies they are not conducting at all. As seen in figure (7a) there is a trend in the shape of the curve with increasing shaliness. In high Q_v samples the clays start contributing to the conductivity at lower salinities. This trend has also been reported by Brown (1988) and Worthington and Johnson (1987).

This effect is present in the bi-modal model as shown in figure (7b). As shaliness increases the fraction of the total porosity due to the clays is larger. In the model the clays conduct within the clay porosity at all salinities. Therefore as the fraction of clays increases, the fraction of the porosity contributed by the clays increases, and the clays can contribute more to the conductivity at lower salinities.

Discussion of clay models

Using PCM the main features of shaly sand conduction have been included in a model based on just the pore structure present in shaly sands. This includes the increase in effective mobility of the clay counter-ions, the increase in m^* with shaliness, and the trend in the shape the C_o-C_w curve with shaliness. It was also demonstrated that the clay geometry can have a dramatic effect on the conductivity.

However, the strength of PCM is that we do not have to be satisfied with average fits to data. For example we can account for mixtures of laminated and dispersed clays. Many times the amounts of dispersed and laminated clays is related to the depositional environment or may be obtained from logs. PCM provides a framework where this type of geologic information may be included in conductivity models with parameters whose meaning is understood.

Summary

A technique has been described for deriving conductivity equations which take into account the lithology and depositional history of rocks. This has been extended from earlier work to include conductive inclusions. Using this equation models were developed for laminated and dispersed clays. These models have the advantage that they allow the effects of clay geometry to be included in the conductivity equations. In this paper we detailed specific models for laminated and dispersed clays, but PCM also provides the framework for developing conductivity models which include even more complicated geologic features. This ultimately should allow models to be modified with a knowledge of changing geology or in some cases to be developed based on just this knowledge.

Nomenclature

σ_h conductivity of the host material

σ_i conductivity of the inclusion

$\sigma_{h,..,k}$ conductivity of the mixture of the host and inclusions h through k, the order of addition follows the ordering of the subscripts.

L_g depolarization ratio of inclusion g

λ_g lithology exponent for inclusion g: $\lambda_g=1/(1-L_g)$

ϕ porosity of the mixture

${}^w\phi_{w,h..,k}$ volume of water normalized to the volume of water and inclusions h through k

V_g volume of inclusion g normalized to the bulk volume

ϕ_g interparticle porosity: ${}^w\phi_{w,g}$

ϕ_m matrix porosity: ${}^w\phi_{w,g,i}$

ϕ_o porosity before the addition of the final component

V_s volume of water, oil and grains normalized to the bulk volume in the laminated clay model

λ_c lithology exponent for the clays: $\lambda_c=1/(1-L_c)$

ϕ_s volume of water and oil normalized to the bulk volume (porosity of the sand) in laminated clay model

λ_{cl} conductivity dependent exponent for laminated clays

λ_{cd} conductivity dependent exponent for dispersed clays

λ_{cs} lithology exponent for the clay sites

σ_n normalized conductivity: $\sigma_n=(\sigma_w-\sigma_i)/\sigma_w$

λ_L geometry dependent lithology exponent: $\lambda_L=1/(1-L\cdot\sigma_n)$

ϕ^{m*} inverse formation factor

ϕ_{cs} porosity of the clay sites: $\phi_{cs}={}^w\phi_{wc}$

$<\lambda_c>$ composite exponent for the clay sites: $<\lambda_c>=\lambda_c\cdot\phi_{cs}^{\lambda cs-1}$

B_{max} maximum equivalent conductivity of the clay counterions

D

SELECTED REFERENCES

1) Myers, M. T., 1989, Log Analyst, to be published

2) Bruggeman, von D.A.G., 1935, Berechnung Vechiedener Physikalischer Konstanten von Heterogenen Substanzen, Ann. Phys. Lpz. Vol.24 pp.636

3) Hanai, T., 1968, Electrical Properties of emulsions, Emulsion Science, ed. by P. Sherman, Acad. Press London, pp. 353

4) Merideth, R.E. and Tobias, C.W.,1962, Advances in Electrochemistry and Electrochemical Engineering, Vol. 2, p.26

5) Sen, P.N., Scala, C., Cohen, M.H., 1981, A self-similar model for sedimentary rocks with application to the dielectric constant of fused glass beads, Geophysics, V46, pp.781

6) Bussian, E. A.,(1983) Electrical Conductance in a Porous Medium., Geophysics, V48, pp.1258

7) Sen, P.N., (1980) The Dielectric and Conductivity Response of Sedimentary Rocks, SPE 9379

8) Swanson, B.F., 1985, Microporosity in Reservoir Rocks-Its Measurement and Influence on Electrical Resistivity, SPWLA, June 17-20.

9) Waxman, M.H. and Smits, L.J.M., Electrical Conductivities in oil-bearing Shaly Sands, Soc. Pet. Engrs J.8, 107-122

10) van Olphen, H. and Waxman M.H., 1958, Surface Conductance of Sodium Bentonite in Water, Proc., Fifth Natl. Conf. Clays and Clay Minerals, NAS-NRC, Pub. 556, 61.

11) Hill, H.J. and Milburn, J.D.,1956, Effect of Clay and Water Salinity on Electrochemical Behavior of Reservoir Rocks, Trans., AIME, Vol19, 649.

12) Waxman M.H. and Thomas, E.C., 1974, Electrical Conductivities in Oil-bearing Shaly Sands: I. The Relation Between Hydrocarbon Saturation and Resistivity Index. II. The Temperature Coefficient of Electrical Conductivity Soc. Pet. Eng J. 14. pp.213-215

13) Brown G.A., 1988 The Formation Porosity Exponent - The Key to Improved Estimates of Water Saturation in Shaly Sands, SPWLA June 5-8

14) Worthington, P.F. Johnson, P.W. 1987, Quantitative evaluation of hydrocarbon saturation in shaly freshwater reservoirs. Trans 16th Annual Convention Indonesian Petroleum Soc.

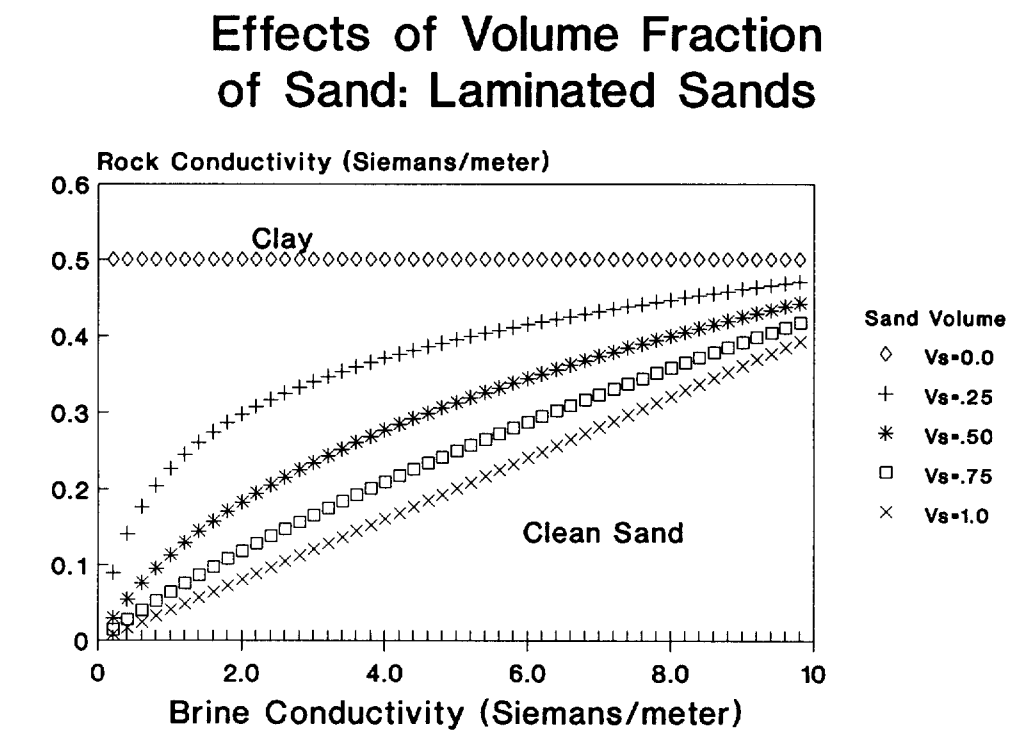

Figure 1a

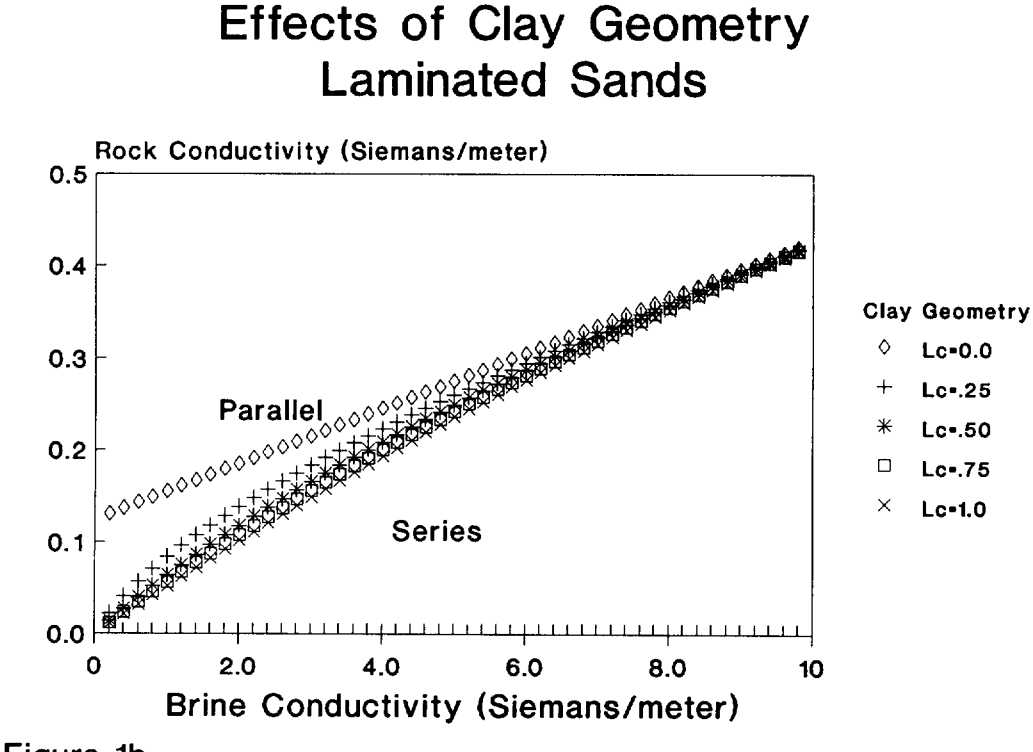

Figure 1b

Effects of Volume of Sand
Laminated Sands

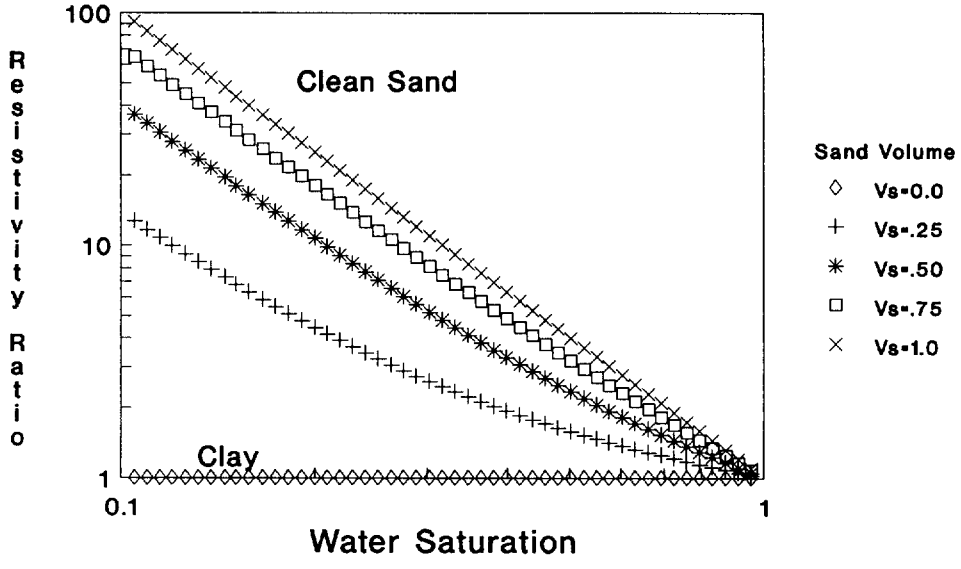

Figure 2a

Effects of Clay Geometry
Laminated Sands

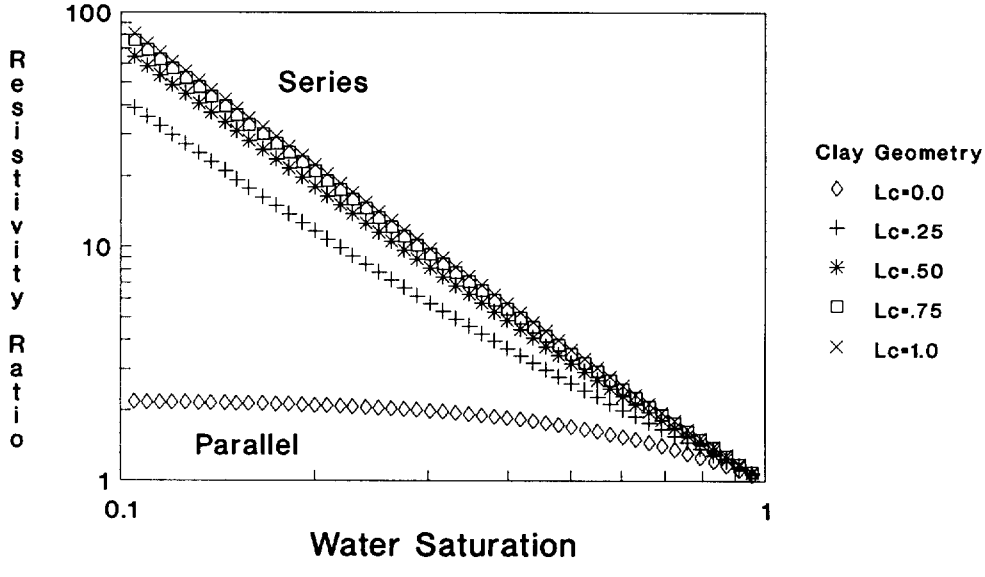

Figure 2b

Effects of Volume of Clay
Dispersed Clays

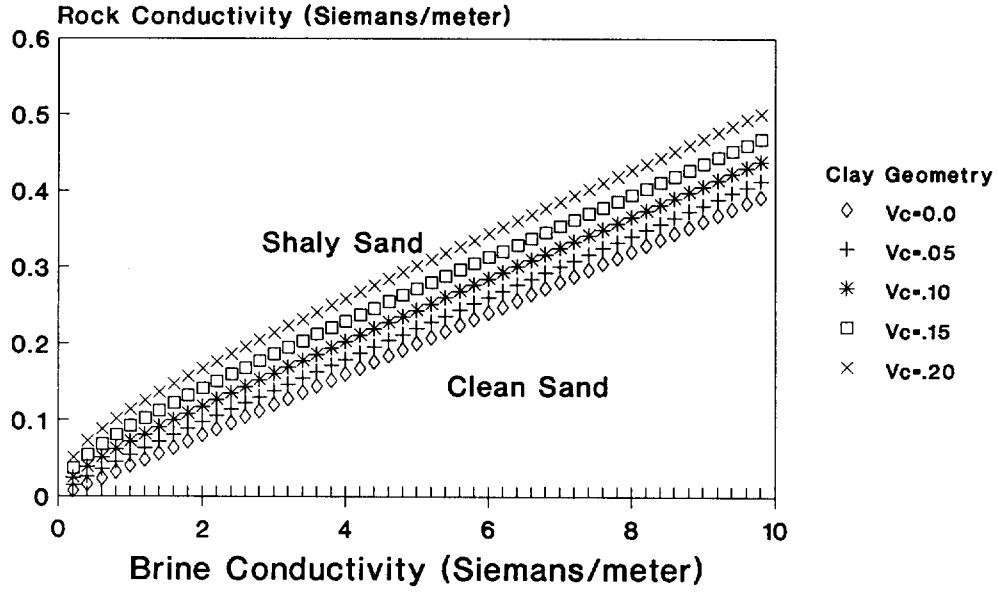

Figure 3a

Effects of Clay Geometry
Dispersed Clays

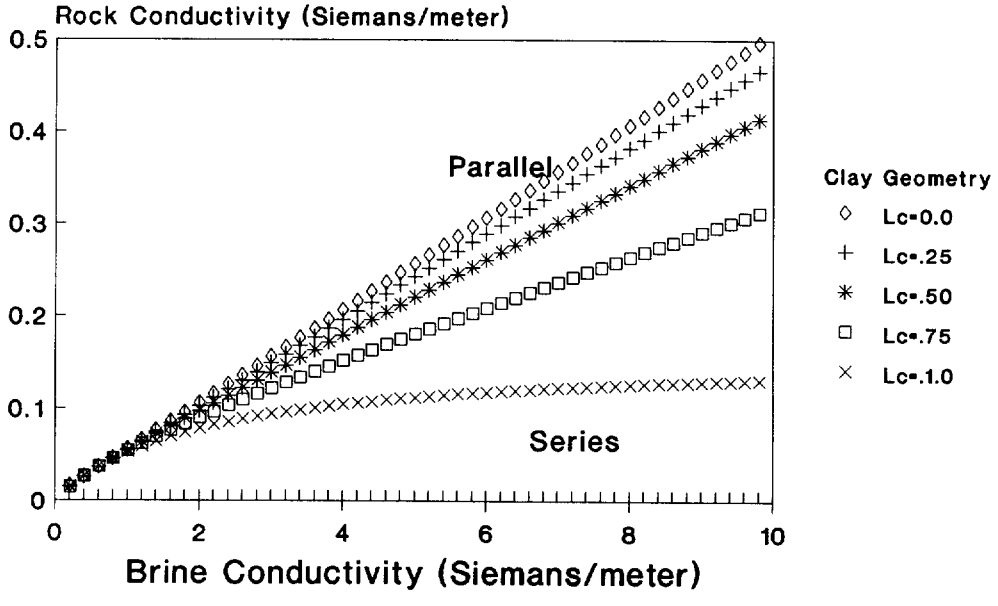

Figure 3b

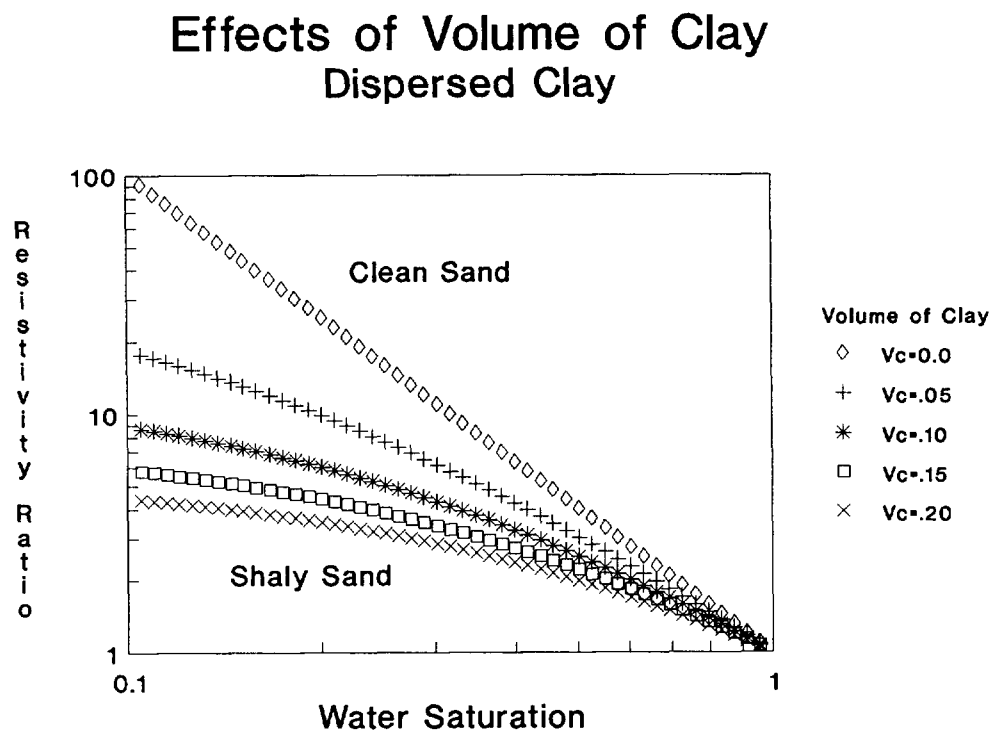

Figure 4a

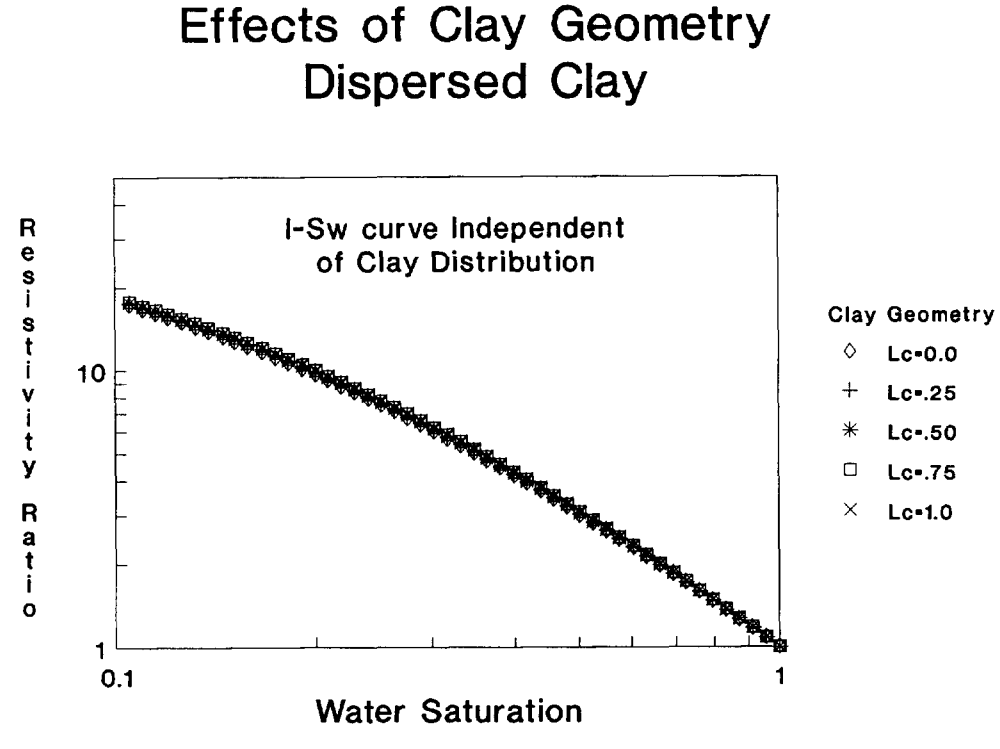

Figure 4b

Trends for Volume Fraction of Clay

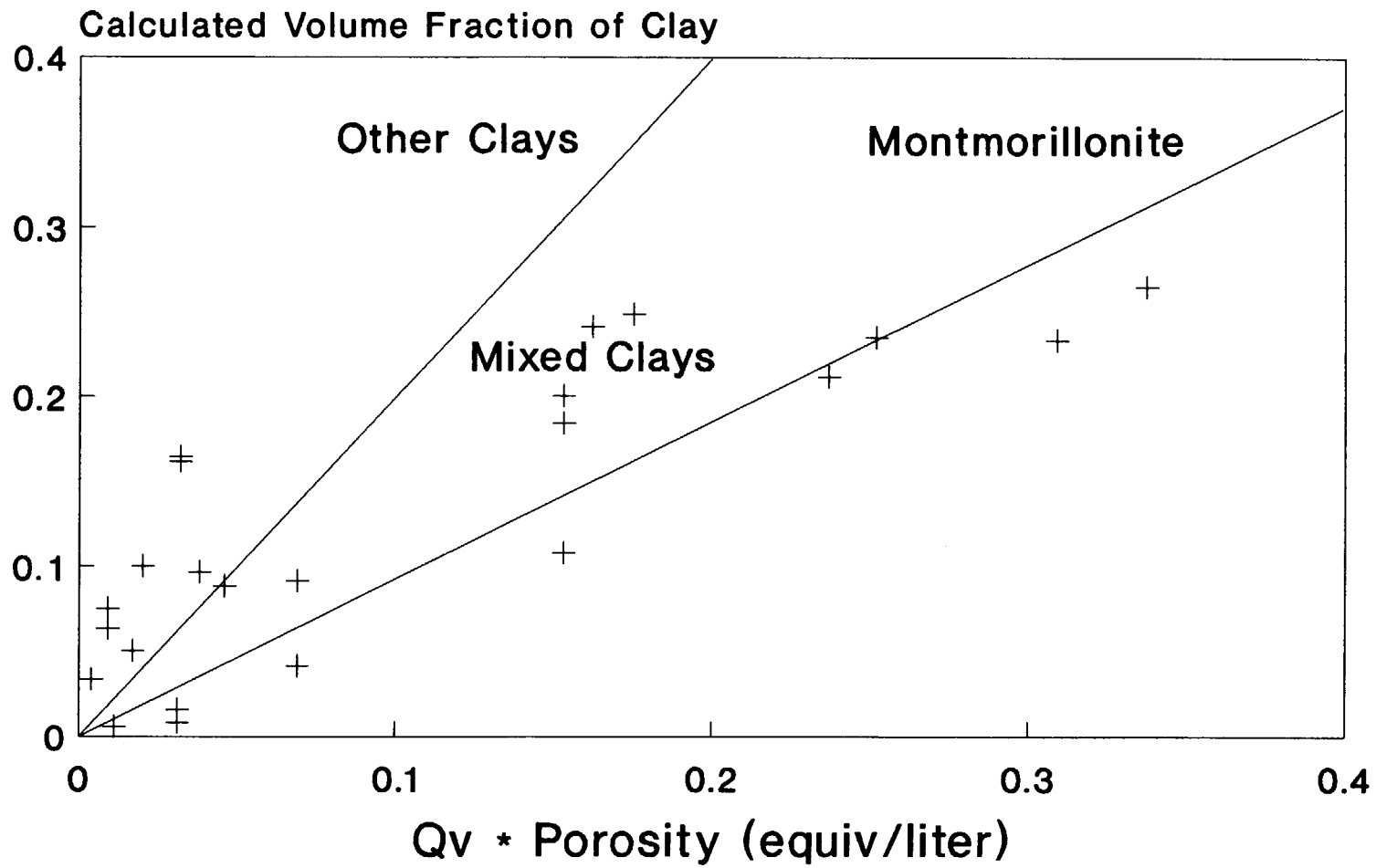

Figure 5

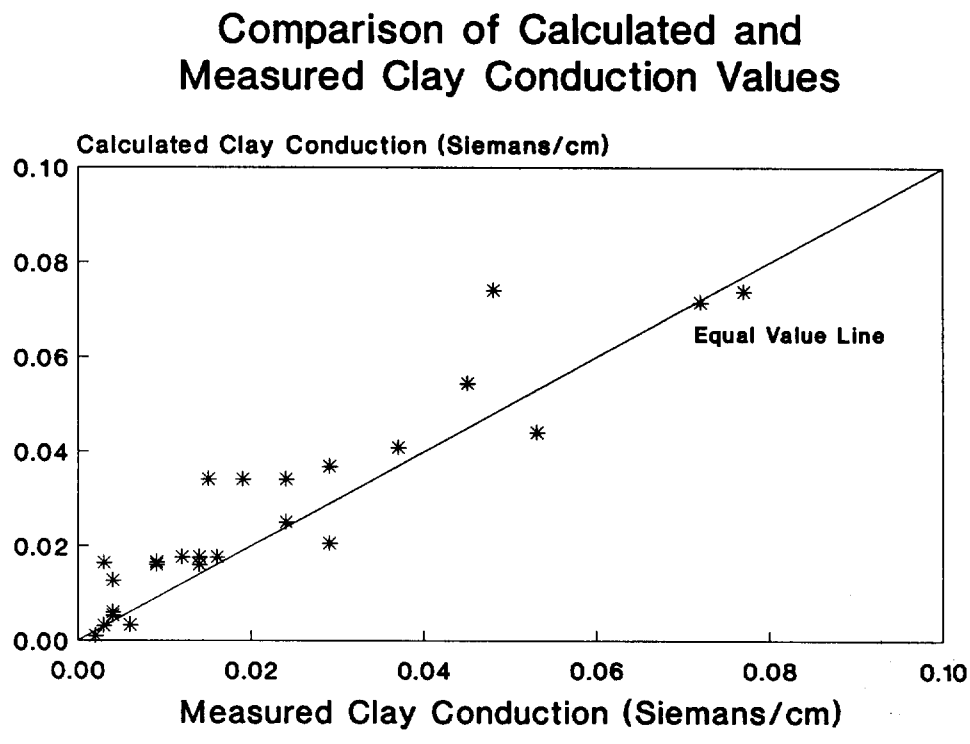

Figure 6a

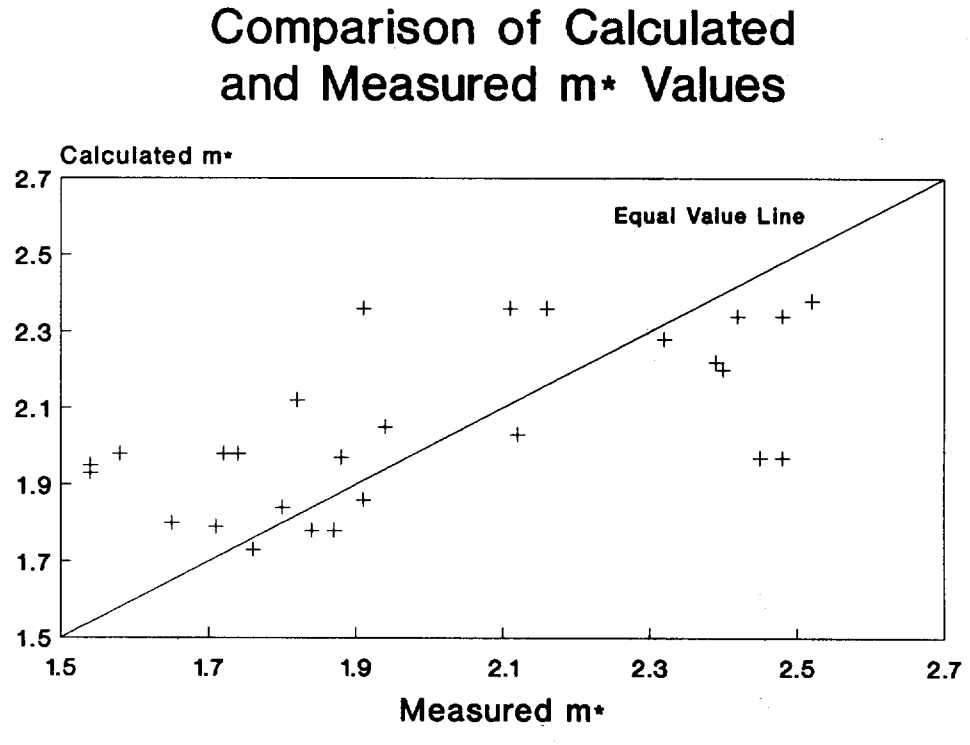

Figure 6b

Trends in Clay Conduction
Kaolinite Samples

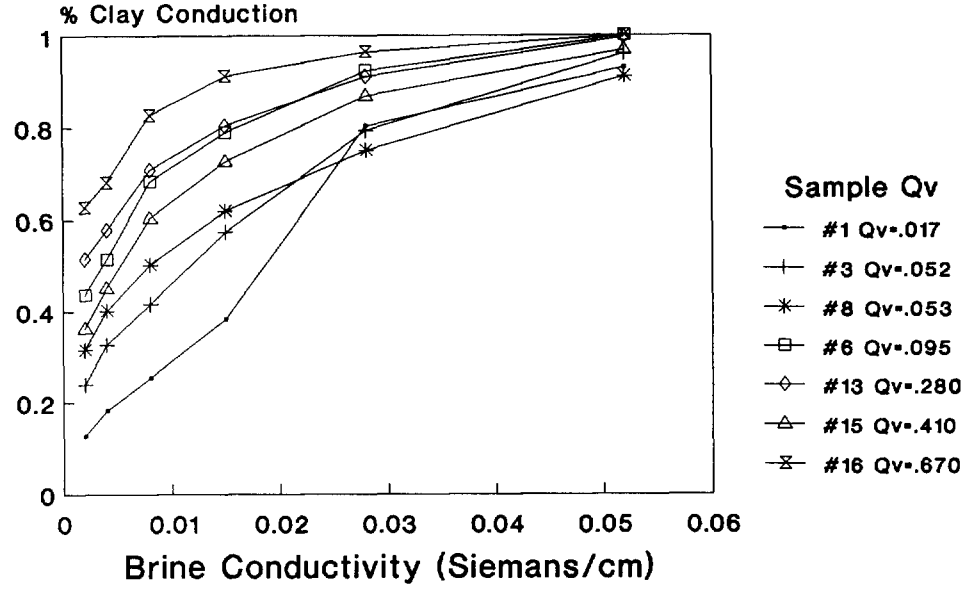

Figure 7a

Calculated Percentage
Clay Conduction

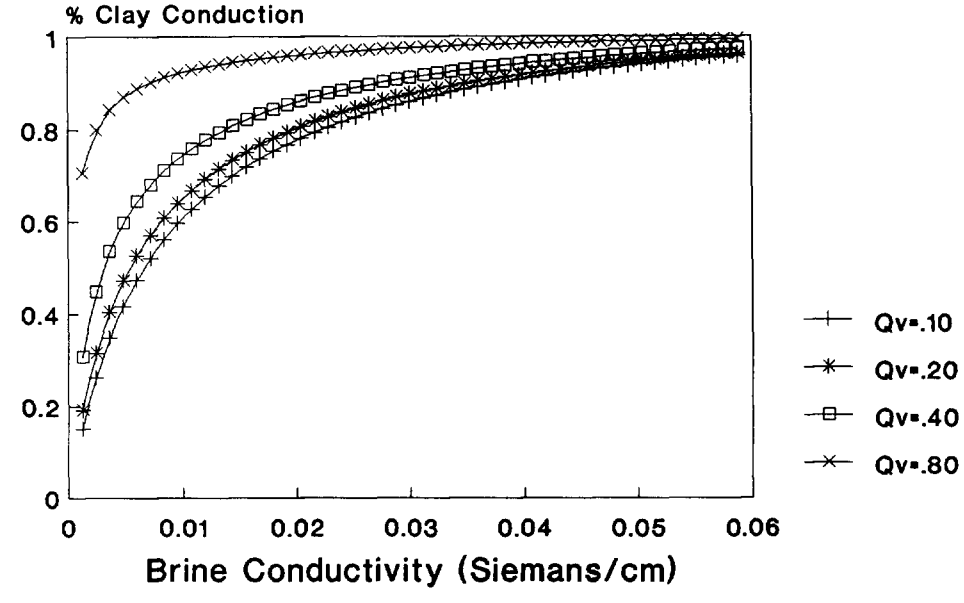

Figure 7b